

## Effect of the Radiation Balance on Warming Occurrence over West Africa

O. S. Ojo<sup>1</sup>, I. Emmanuel<sup>2</sup>, B. Adeyemi<sup>3</sup> and E. O. Ogolo<sup>4</sup>

<sup>1,2,3,4</sup>Atmopheric Research Group, Department of Physics, P.M.B. 704, The Federal University of  
Technology, P.M.B. 704, Akure, Nigeria

Corresponding Author: Olusola Ojo ([ojoso@futa.edu.ng](mailto:ojoso@futa.edu.ng))

ORCID ID: [0000-0003-0958-9790](https://orcid.org/0000-0003-0958-9790)

### Key Points

1. The study reveals decrease in radiation balance flux over West Africa which is an indication of increase in surface temperature.
2. The study shows near extreme warming events over entire West Africa considering the trends and values of climate warming indices.
3. The cross-correlation analysis carries out between radiation balance flux and warming indices in this study shows strong sensitivity.

# Effect of the Radiation Balance on Warming Occurrence over West Africa

O. S. Ojo<sup>1</sup>, I. Emmanuel<sup>2</sup>, B. Adeyemi<sup>3</sup> and E. O. Ogolo<sup>4</sup>

<sup>1,2,3,4</sup>Atmospheric Research Group, Department of Physics, P.M.B. 704, The Federal University of Technology, P.M.B. 704, Akure, Nigeria

Corresponding Author: Olusola Ojo ([ojoso@futa.edu.ng](mailto:ojoso@futa.edu.ng))

ORCID ID: [0000-0003-0958-9790](https://orcid.org/0000-0003-0958-9790)

## Abstract

In this study, daily atmospheric radiation and temperature data at the surface were obtained from the archives of the Modern-Era Retrospective Analysis for Research and Applications, Version 2 (MERRA-2) for the period of 36 years (1980 – 2015) over West African geo-climatic regions. Analyses showed that the values of radiation balance in entire West Africa decreased from  $140.37 \pm 2.11 \text{ W/m}^2$  in 1980 to  $132.89 \pm 2.18 \text{ W/m}^2$  in 2015. This shows that there is dominance of longwave radiation components in the radiation balance budget which determines the warming effect in the earth surface. Also, the magnitudes of ratio of change in surface temperature to change in radiation balance flux (radiative forcing) termed climate sensitivity ranged between  $1.74 \pm 0.08$  and  $3.92 \pm 0.69$  across the studied regions. These values fall within the threshold values of 1.5 and 4.5 proposed by the Intergovernmental Panel on Climate Change (IPCC) Assessment Report for the prevalence of surface warming. Meanwhile, the trend analyses of frequencies and intensities of warm nights and warm days whose maximum values were  $35.52 \pm 0.77 \text{ }^\circ\text{C}$  and  $42.34 \pm 0.73 \text{ }^\circ\text{C}$  showed predominant significant increasing trends respectively. Also, cross correlation analysis reveals strong significant relationships between radiation balance flux and temperature extreme events at short time-lags. Finally, it can be inferred from the results that the climate system of the West African Region is experiencing warming effects in which radiation balance contributed significantly. Consequently, this may result in more heat stress, drought, and flooding causing negative influences on agriculture, forestry, and entire ecosystems in this 21<sup>st</sup> century.

**Keywords:** Warming occurrence; MERRA-2 data; Radiation balance; Climate sensitivity; Extreme event; West Africa

## 1 Introduction

Radiation balance is the distinction between the energy radiated from the sun known as shortwave radiation and the energy emitted from the earth's surface known as longwave radiation at earth's surface. It is the amount of energy available to drive climate processes such as evapotranspiration, sensible heat exchange, and elements of the carbon cycle, such as plant metabolism and photosynthesis. The imbalance in emission of longwave radiation and shortwave radiation gives significant feedbacks to the evolution of global climate systems (Sai Krishna et al. 2014). It determines the thermal structure as well as the dynamics of the atmosphere. It is mostly influenced

by the surface albedo, clouds, aerosols, greenhouse gases, and ozone (Chen et al. 2016, Saud et al. 2016, Liang et al. 2018). The long-term change in radiative fluxes imbalance gives rise to net radiative forcing. The linear relationship between changes in surface temperature and net radiative forcing is known as climate sensitivity (Gregory et al. 2002, Gregory et al. 2004, Rohling et al. 2012). This evaluates how sensitive is the global climate to the amount of energy reaching the earth's surface (Meehl et al. 2007, Rahmstorf 2008, Tung et al. 2008). Climate sensitivity is an essential parameter that accounts for the feedbacks from gradual increase in surface temperature over a long period of time, that is global warming. The Intergovernmental Panel for Climate Change (IPCC) Fifth Assessment Report (AR5) in 2013, proposed the threshold value of climate sensitivity to be extremely unlikely less than 1, likely between 1.5 and 4.5 and very unlikely greater than 6 by 2100. The feedbacks of global warming cause precipitation changes, storm intensity and tracks, El Nino, and even ocean circulation which are principal signatures of climate change (Maslin, 2008).

Climate change can be defined as the periodic modification of Earth's climate over time. It reflects changes in the variability or average state of the atmosphere over time scales ranging from decades to millions of years (Hansen and Sato 2012). The direct consequence of climate change is global warming which can lead to the occurrence of flooding, drought and heatwaves as well as land degradation with resultant impacts on food security and mortality rate of livestock (Laurance and Williamson 2001, 2001, 2001, Lal 2004, Jackson et al. 2011). It can manifest itself in several ways such as changes in regional and global temperatures, changing rainfall patterns, expansion, and contraction of ice sheets, and sea-level variations. These regional and global climate changes are responses to external and/or internal forcing mechanisms. The example of an internal forcing mechanism is the variations in the carbon dioxide content of the atmosphere modulating the greenhouse effect, while a good example of an external forcing mechanism is the long-term variations in the Earth's orbits around the sun, which alter the regional distribution of solar radiation to the Earth. West Africa has been identified as a climate change hotspot because of the increase in anthropogenic activities due to high population growth and urbanization of in the region (Ojo et al. 2019). The anthropogenic activities lead to an increase in the greenhouse gases and these, in turn, increases the amount of longwave radiation that can be absorbed and therefore the amount that can be re-emitted back to warm up the Earth (Maslin 2004). The major indicator of climate change is the long-term changes in extreme climate events obtained from daily temperature and precipitation (Folland et al. 2001, Aguilar et al. 2009). The lists of these climate extremes are presented in Table 1. Some scientists have observed that changes in climate extremes have more impacts than changes in mean values of temperature and precipitation on human and natural systems (Folland et al. 2001, Aguilar et al. 2009, Zhang and Zhai 2011). A changing climate leads to changes in the frequency, intensity, spatial extent, duration, and timing of weather and climate extremes, and can result in unprecedented extremes (Nicholls et al. 2012).

Furthermore, it has been established in literature that the climate change is dependent on the intensity of radiative forcing because the radiative response is proportional to the surface temperature, one of the key elements of climate change (Schwarzkopf and Ramaswamy 1993,

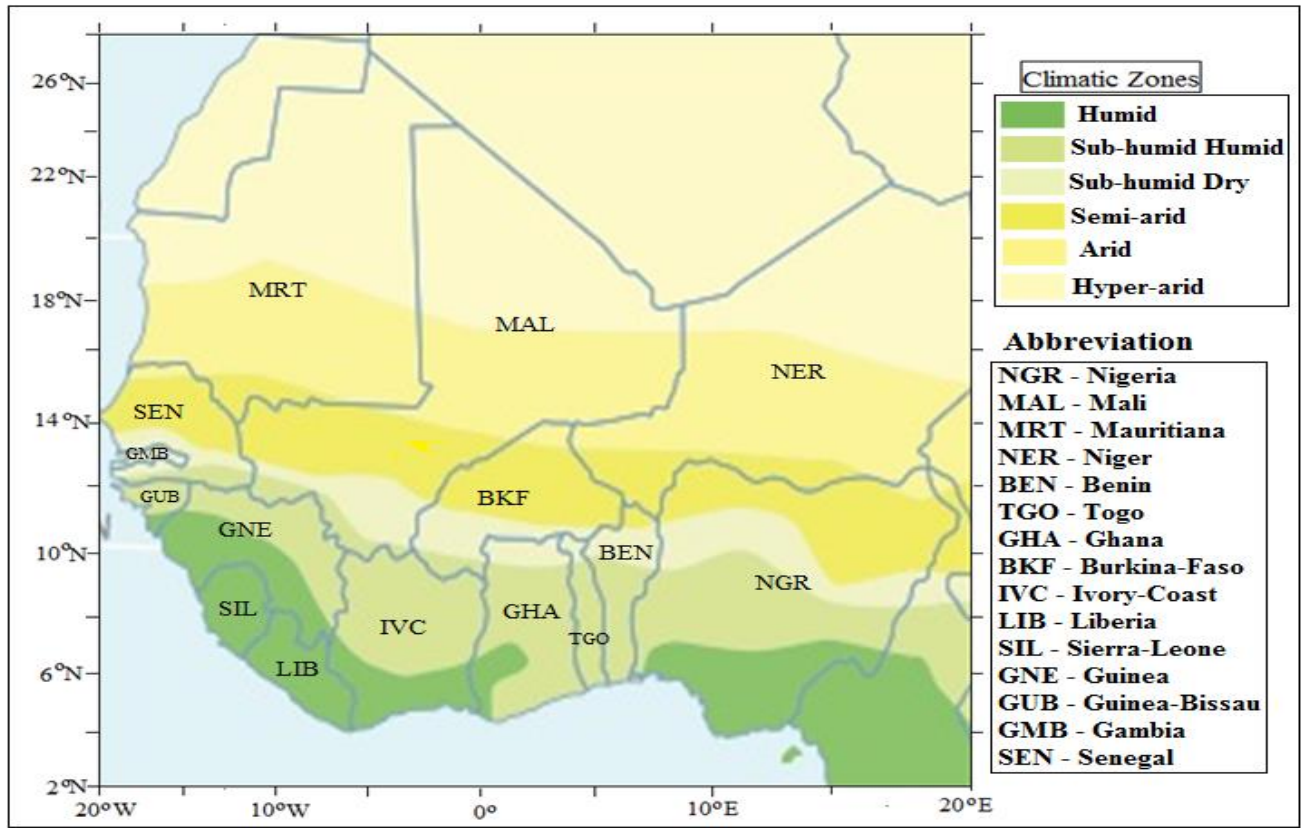
Houghton et al. 1995, Gregory et al. 2004). The intensity of radiative forcing either positive or negative feedback is caused by the degree of concentration of the emission of greenhouse gases as well as the extent of land-use and land-cover (Dickinson and Cicerone 1986, Hansen et al. 2000, Andres et al. 2012). Meanwhile, Nicholls et al.(2012) studied the changes in climate extremes and their impact on the physical environment globally. The study found that there were decreased in frequencies of cold days, cold nights, and cold spells but the frequencies of warm days, warm nights, and warm spells showed increasing trends on the global scale. Also, a strong significant increase in trends was observed in the case of heavy precipitation events in the study. Trenberth et al.(2014) studied energy imbalance on the Earth's surface and observed that net energy imbalance varies naturally in response to weather and climate variations. The study concluded that these influenced the climate change signals associated with changes in atmospheric composition. Gadea Rivas et al.(2017) investigated the existence of global warming using the trends in distributional characteristics (moments and quartiles) of the global temperatures for the period of 1770-2017 from Central England and 1880-2015 from global sectional temperatures. The study concluded that there was an increasing trend in all distributional characteristics (time series and cross-sectional). However, the biggest problem with the global warming hypothesis is understanding how sensitive and responsive the global climate is to increased levels of atmospheric carbon dioxide, radiative forcing, and extreme events. This present study tends to solve this problem by investigating the evolution of surface warming across West Africa using climate sensitivity and trends in climate extreme events. The relationship between radiation balance and climate extreme events was evaluated using cross-correlation method. This method has been used extensively to evaluate the relationship between rainfall and streamflow (Croke et al. 2015, Menke and Menke 2016), pressure and four state indicators of the fish population (Probst et al. 2012, 2012), trace N<sub>2</sub>O concentration and meteorological data (Kamata et al. 2002), precipitation and temperature in the simulation of the hydrological cycle (Seo et al. 2019, 2019) and neighborhood-level vulnerability to climate change and protective green building design strategies (Houghton and Castillo-Salgado 2020). The results obtained will serve as working tools for the inter-governmental climate agencies and stakeholders for decision-making.

## **2 Data Analyses Techniques**

Atmospheric data of daily atmospheric radiations and temperature taken over West Africa were obtained from the archives of Modern-Era Retrospective Analysis for Research and Applications, Version 2 (MERRA-2) for the period of 36 years (1980 – 2015). MERRA-2 provides reanalysis meteorological data derived from GOES-5 satellite and GPS-Radio Occultation dataset beginning from 1980 up to date at different timescales using the resolution of  $0.5^{\circ} \times 0.66^{\circ}$  grid with 72 layers. Surface data obtained include atmospheric radiation components (incoming and outgoing shortwave, incoming and outgoing longwave radiation) and climate parameters such as minimum temperature, maximum temperature, and precipitation. Net Radiation (Q) at the surface was computed using:

130 
$$Q = (S \downarrow - \alpha S \uparrow) + (L \downarrow - L \uparrow) \quad (1)$$

131 where  $S \downarrow$  is the incoming shortwave radiation ( $W/m^2$ ),  $S \uparrow$  is the outgoing shortwave radiation  
 132 ( $W/m^2$ ),  $L \downarrow$  is the incoming longwave radiation ( $W/m^2$ ),  $L \uparrow$  is the outgoing longwave radiation  
 133 ( $W/m^2$ ) and  $\alpha$  is the surface albedo. West Africa grouped into six climatic zones following the  
 134 classification of the World Meteorological Organization based on the latitudinal ranges, which  
 135 include: Hyper-Arid Zone (HAR) ( $20^\circ N$ ,  $28^\circ N$ ); Arid Zone (ARD) ( $17^\circ N$ ,  $20^\circ N$ ); Semi-Arid Zone  
 136 (SAR) ( $13^\circ N$ ,  $15^\circ N$ ); Sub-humid Dry Zone (SHD) ( $15^\circ N$ ,  $16^\circ N$ ); Sub-humid Humid Zone (SHH)  
 137 ( $11^\circ N$ ,  $13^\circ N$ ); and Humid Zone (HUM) ( $5^\circ N$ ,  $12^\circ N$ ) as shown in Figure 1.



138  
 139 Figure 1: A Map of West Africa showing the investigated Climatic Zones and their respective  
 140 countries (Source: OECD, 2007, 2008a; WMO, 2011),

141 In addition, climate sensitivity was evaluated using the linear relationship between radiative forcing  
 142 ( $\Delta Q$ ) and the surface temperature ( $\Delta T$ ) according to Drakes (2000) as:

$$\Delta T = \Phi \Delta Q \quad (2)$$

143 where  $\Phi$  is the climate sensitivity in kelvin per watts per square metres which accounts for feedback  
 144 of global warming (Houghton et al. 1995, Drake 2000, Lin et al. 2011).

Also, eight temperature extreme indices over the six climatic regions in West Africa from 1980 to 2015 were computed using the surface data of daily minimum and maximum temperature and precipitation series. They were selected from the lists of core climate extreme indices recommended by the World Meteorological Organization – Commission for Climatology (WMO-CCL) and the research project on Climate Variability and Predictability (CLIVAR) of the World Climate Research Programme (WCRP) as adapted from Keggenhoff et al.(2014) and You et al.(2011). These indices (see Table 1) were used to investigate the warming potential over West Africa.

Table 1: Climate Extreme Indices selected for the study (Source: Keggenhoff et al.(2014) )

Indices	Index	Description Name	Definition	Unit
Temperature	Tn10p	Cold Nights Frequency	Percentage of days when Tn < 10th percentile of 1980 – 2015	%
	Tx10p	Cold Days Frequency	Percentage of days when Tx > 10th percentile of 1980 – 2015	%
	Tx90p	Warm Days Frequency	Percentage of days when Tx > 90th percentile of 1980 – 2015	%
	Tn90p	Warm Nights Frequency	Percentage of days when Tn > 90th percentile of 1980 – 2015	%
	Tnn	Coldest Night	Annual lowest Tn	°C
	Tnx	Warmest Night	Annual highest Tn	°C
	Txn	Coldest Day	Annual lowest Tx	°C
	Txx	Warmest Night	Annual highest Tx	°C

**Note: Tx is daily maximum temperature, Tn is daily minimum temperature.**

Meanwhile, the presence of a monotonic increasing or decreasing trend in the climate variables  $S$  between 1980 and 2015 was tested with the nonparametric Mann-Kendall test (Gilbert 1987, Ogolo and Adeyemi 2009). The variance of  $S$  was computed using Equation (3) which takes the presence of ties into account:

$$Var(S) = \frac{1}{18} \left[ n(n-1)(2n+5) - \sum_{p=1}^a t_p(t_p-1)(2t_p+5) \right] \quad (3)$$

where  $p$  is the number of tied groups and  $t_p$  is the number of data values in the  $p$ th group.

$$Z = \begin{cases} \frac{S-1}{\sqrt{VAR(S)}} & \text{if } S > 0 \\ 0 & \text{if } S = 0 \\ \frac{S+1}{\sqrt{VAR(S)}} & \text{if } S < 0 \end{cases} \quad (4)$$

A positive or negative value of  $Z$  indicates an upward or downward trend of the studied variables respectively. All significant trends were evaluated at 0.05 alpha level of significance.

Furthermore, cross-correlation function was used to analyze the time-lagged relationships between radiation balance fluxes and climate extreme events to assess their sensitivity and responsiveness to each other. Sensitivity is quantified as the strength of the peak cross-correlation in the CCF while responsiveness is then quantified as the lag of this CCF peak (Rice and Rochet 2005, Probst et al. 2012). Theoretically, the cross-correlation between the time-series  $Y$  and  $X$  can be expressed by the ratio of covariance to root-mean variance according to Boyd (2001) as:

$$\rho_{y,x} = \frac{\gamma_{y,x}}{\sqrt{\sigma_y^2 \sigma_x^2}} \quad (5)$$

where  $\rho$  is the cross-correlation function of the two time-series,  $\gamma$  is the covariance of the two time-series,  $\sigma^2$  is the standard deviation of time-series  $Y$  and  $X$ . The covariance between  $Y$  and  $X$  time-series is given by:

$$\gamma_{y,x} = \frac{1}{N} \sum_{i=0}^N (Y - X)(X - Y) \quad (6)$$

Cross-correlations are dimensionless, ranging in value from -1.0 to +1.0. In this study,  $Y$  represents radiation balance fluxes time-series ( $Q_n$ ,  $Q_x$ , and  $Q$ ) while  $X$  represents temperature time-series ( $T_{n10p}$ ,  $T_{n90p}$ ,  $T_{nn}$ ,  $T_{nx}$ ,  $T_{x10p}$ ,  $T_{x90p}$ ,  $T_{xn}$ ,  $T_{xx}$ ) and precipitation indices time-series ( $R_{20mm}$ ,  $R_{95p}$ ,  $SDII$ ,  $CDD$ ). These variables were detrended and prewhitened in order to make them stationary for cross-correlation analyses using the methods proposed by (Cryer and Chan 2008, Gröger et al. 2010, Gröger and Fogarty 2011, Song 2017).

### 3 Results and Discussion

#### 3.1. Spatial Distribution of Radiation balance flux and Climate Sensitivity over West Africa and their Trends

##### *Spatial Distribution*

Figure 2 (a-c) shows the spatial distributions of radiation balance fluxes sandwiched with their trends over West Africa for the nighttime, daytime, and daily average for 1980 and 2015. The figures showed that net radiation increases as the latitude decreases, that is, it has lower values in the arid zones and higher values in the humid zones for the three timeseries. The variability in the surface albedos which are lower in humid zones and higher in arid zones may be responsible for this observation. The patterns of distribution of daytime net radiation are similar to that of average values (Figures 2b and 2c) showing that daytime net radiation is more sensitive to the daily average. The minimum, maximum, mean and other statistical values that describe the magnitudes of nighttime,

daytime, and daily average radiation balance flux are presented in Table 2. This indicates that more energy will be available for atmospheric processes and consequently there may be possibility of warming effects in the zones.

On the other hand, the effect of net radiation on climate warming event was investigated using climate sensitivity in terms of change in net radiation as shown in Figures 3. Figure 3 (a) shows the spatial distributions of climate sensitivity sandwiched with its trends over West Africa. The figure showed that values of climate sensitivity increased from the coast inland. That is, higher values were discernible in the arid zone having maximum value of  $3.92 \pm 0.17 \text{ K/W/m}^2$  in the northern areas of Mali, Mauritania and Niger Republic. The lower values were found in the humid zones having minimum value of  $1.74 \pm 0.04 \text{ K/W/m}^2$  in the coastal areas of Nigeria, Ghana and Sierra-Leone. The distribution of standard deviation of climate sensitivity ranging from  $0.04 \text{ K/W/m}^2$  to  $0.17 \text{ K/W/m}^2$  was shown in Figure 3(b). The figure revealed higher variability in the humid zones. Comparing these results with IPCC threshold values of 1.5 to 4.6, the entire regions of West Africa are experiencing surface warming conditions. The descriptive statistics of climate sensitivity are shown in Table 2.

### ***Trend Analysis***

Also, the trend test revealed that radiation balance flux showed both significant increasing and decreasing trends across the zones over West Africa. For nighttime net radiation ( $Q_n$ ), the majority of the trend tests showed increasing trends in which almost one-third of them are significant in western areas such as Senegal, Gambia, Guinea coasts (Figures 2(a) and Table 5b). However, daytime and daily average net radiation ( $Q_x$  and  $Q$ ) showed decreasing trends in which the majority were significant as shown in Figures 2(b), 2(c), and Table 5a. The prevalence of increasing trends for  $Q_n$  and decreasing trends for  $Q_x$  and  $Q$  showed that there was a predominant influence of longwave radiation component in radiation budget especially outgoing longwave radiation (OLR). OLR is one of the major factors



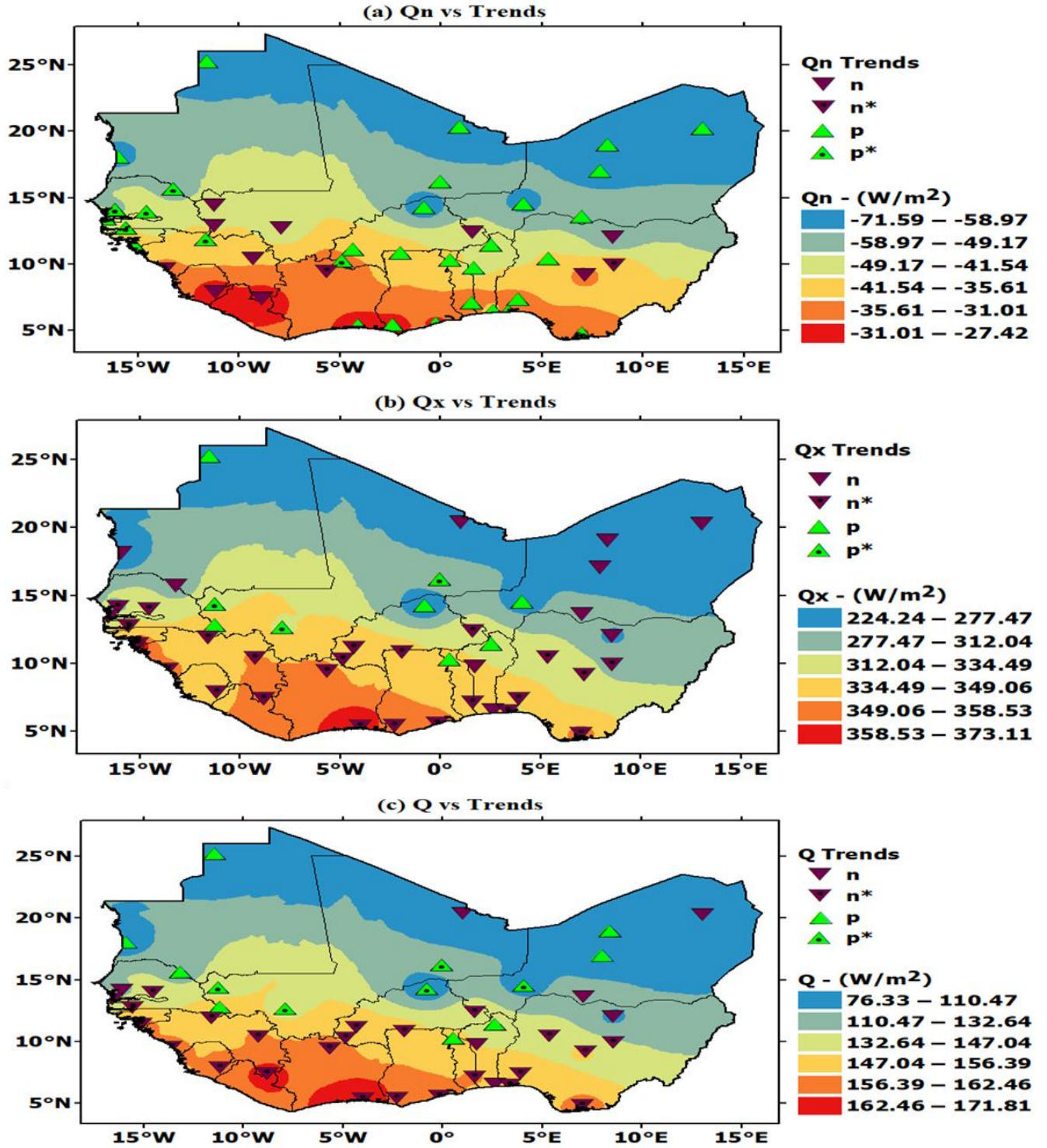
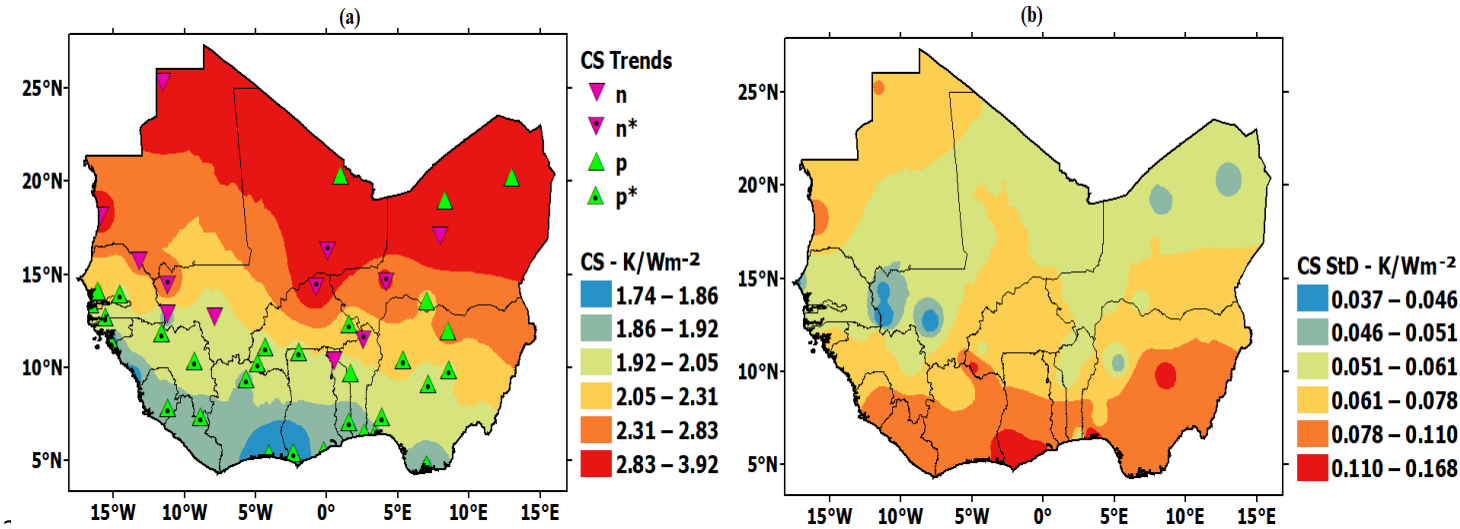


Figure 2: Spatial Distributions of (a) Nighttime Net Radiation (Qn) (b) Daytime Net Radiation (Qx) (c) Annual Mean Net Radiation Sandwiched with their Respective Trends over West Africa. (Note: n = negative trends, n\* = negative trends significance at 0.05 alpha level, p = positive trends, p\* = positive trends significance at 0.05 alpha level).

218 Table 2: Descriptive Statistics of Radiation Balance Flux and Climate Sensitivity for the Period of 1980 and  
219 2015 over West African Zones

Variable	Zone	Minimum	Maximum	Mean	Standard Deviation	10th Percentile	90th percentile	Kurtosis	Skewness
Nighttime Radiation Balance Flux	HAR	-72.55	-66.8	-69.69	1.46	-71.47	-67.4	-0.82	0.24
	ARD	-65.82	-57.69	-62.64	1.99	-65.17	-59.71	-0.47	0.5
	SAR	-57.12	-47.45	-52.16	2.26	-55	-49.12	-0.17	-0.01
	SHD	-47.07	-36.81	-41.16	2.3	-44.48	-38.11	0.83	-0.58
	SHH	-40.5	-31.29	-34.99	1.92	-37.05	-32.4	1.44	-0.64
	HUM	-33.77	-28.74	-30.71	1.14	-32.37	-29.44	0.49	-0.8
Daytime Radiation Balance Flux	HAR	220.74	228.84	225.21	2.4	221.38	228.54	-0.96	-0.22
	ARD	246.9	262.36	254.12	3.73	248.53	259.09	-0.37	-0.01
	SAR	295.63	314.29	306.29	4.92	300.28	312.98	-0.55	-0.3
	SHD	321.67	344.91	334.01	6.86	323.51	343.25	-0.93	-0.27
	SHH	329.21	363.94	347.59	9.87	333.73	361.65	-0.99	-0.02
	HUM	324.44	381.93	352.5	16.61	329.93	374.92	-1.22	0.01
Daily Radiation Balance Flux	HAR	75.39	79.92	77.76	0.99	76.48	79.16	0.22	0.04
	ARD	92.14	99.24	95.74	1.74	93.33	98.25	-0.37	-0.03
	SAR	122.56	131.14	127.06	2.22	123.96	130.32	-0.61	0.12
	SHD	140.35	151.83	146.43	3.2	141.81	150.53	-1.15	-0.18
	SHH	146.19	163.92	156.3	5.02	149.98	163.19	-1.08	-0.02
	HUM	145.64	175.29	160.9	8.46	149.13	172.27	-1.21	-0.04
Climate Sensitivity	HAR	3.74	3.97	3.85	0.05	3.78	3.91	0.11	-0.12
	ARD	3.04	3.27	3.15	0.06	3.07	3.23	-0.39	0.05
	SAR	2.30	2.46	2.38	0.04	2.32	2.43	-0.59	-0.05
	SHD	1.94	2.10	2.02	0.04	1.96	2.08	-1.11	0.24
	SHH	1.83	2.06	1.93	0.06	1.85	2.01	-1.02	0.12
	HUM	1.71	2.06	1.86	0.10	1.74	2.01	-1.16	0.19

220



222 Figure 3: Spatial Distributions of (a) Climate Sensitivity (CS) (b) Standard Deviation of Climate Sensitivity  
223 over West Africa

224

225 that contributed to an increase in the surface temperature leading to global warming and the  
226 alteration of the hydrological cycle (Rannow and Neubert 2014, Boudiaf et al. 2020) . In the same  
227 vein, predominant significant increasing trends were detected for climate sensitivity as shown in  
228 Figure 4a and Table 5a. It should be noted that the majority of the significant increasing trends were  
229 found in the humid zones. This may be attributed to the high degrees of anthropogenic activities in  
230 these areas. The few decreasing trends were detected at the centre of arid zones. Less anthropogenic  
231 coupled with desertification may be responsible for this observation. These are the signature of  
232 climate change that may cause drought, rise in sea level, and flooding which are inimical to human  
233 existence, agricultural productivity, and economic boost.

### 234 **3.2. Spatial Distributions and Trend tests of Temperature Extreme Events**

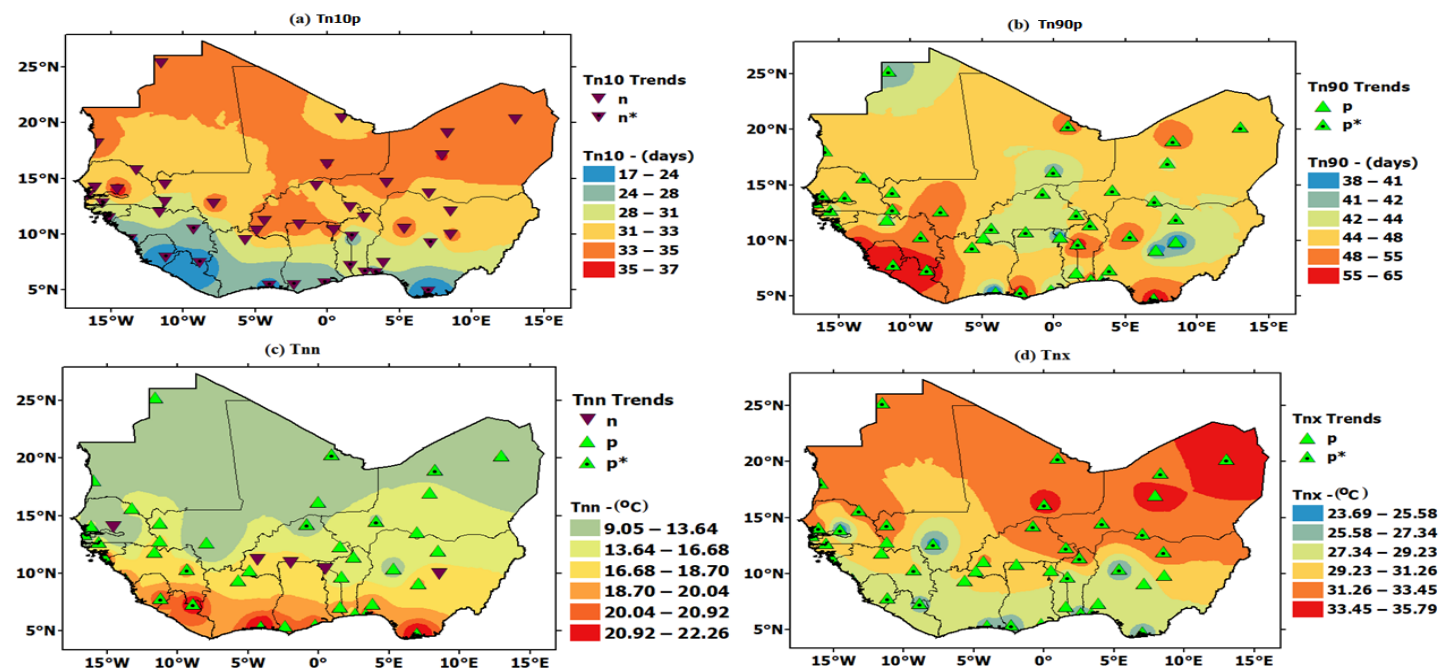
#### 235 *Spatial Distributions*

236 Furthermore, Figures 4 (a-d) and 5 (a-d) present the spatial distributions of nighttime and daytime  
237 temperature extreme events sandwiched with their respective trends represented by small triangular  
238 symbols over West Africa. Figures 5a and 6a showed that cold nights (Tn10p) and Cold days (Tx10)  
239 frequencies increased from the Humid zones to the Arid zones, that is, along increasing latitudes.  
240 Numerically, Tn10p and Tx10p have maximum magnitudes of 37 days and 38 days in the Arid  
241 zones while the minimum magnitudes are 17 days and 18 days in the humid zones as the annual  
242 daily average respectively. Conversely, the distributions of warm nights (Tn90) and warm days  
243 (Tx90) frequencies have similar irregular patterns which are almost decreased along with an increase  
244 in latitudes, that is, decreased from the Humid zones to the Arid zones. Tn90p and Tx90p have  
245 maximum magnitudes of 65 days and 62 days while the minimum magnitudes are 38 days and 30  
246 days as the annual daily average respectively (Figures 4b and 4b). Also, the distributions of coldest  
247 nights (Tnn) and coldest days (Tnx) temperatures were observed to increase in magnitudes along  
248 decreasing latitudes, that is, increase from the Arid zones to the humid zones (Figures 4c and 5c).  
249 Tnn and Tnx have maximum magnitudes of 22.26 °C and 53.71 °C in the Humid zones while the  
250 minimum magnitudes are 9.05 °C and 16.02 °C in the Arid zones as the annual daily average  
251 respectively. However, the distributions of warmest nights (Tnx) and warmest days (Txx)  
252 temperatures were observed to increase in magnitudes along increasing latitudes, that is, increase  
253 from the Humid zones to the Arid zones (Figures 4d and 5d). Tnx and Txx have maximum  
254 magnitudes of 35.79 °C and 63.89 °C while the minimum magnitudes are 23.69 °C and 23.89 °C as  
255 the annual daily average respectively. The regional descriptive statistics of the temperature extreme  
256 indices were presented in Tables (3 – 4).

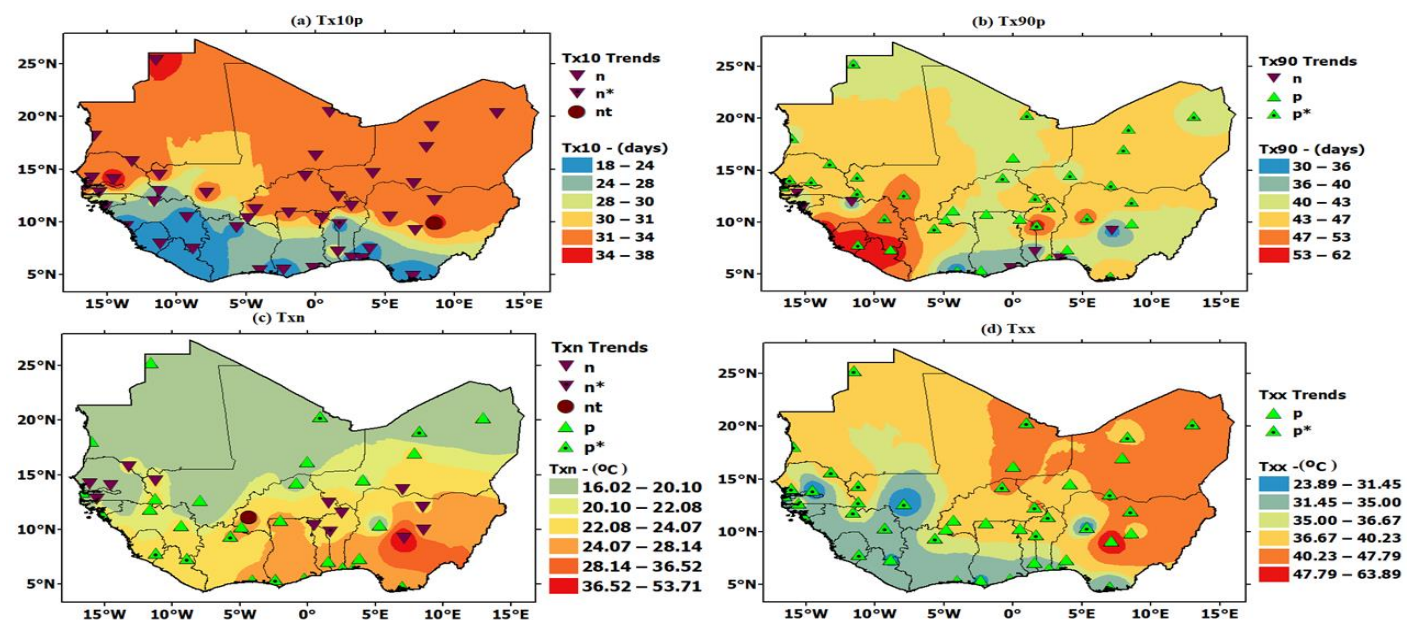
#### 257 *Trends Analyses*

258 In the same vein, predominant decreasing trends were detected for both Tn10p and Tx10p as shown  
259 in Tables 5 (a-b). All the significant decreasing trends detected in Tn10p were found in the coastal  
260 areas in West Africa (Figure 4a) while the only significant decreasing trends detected for Tx10p

261 were found in the western part of the Benin Republic (Figure 5a). On the regional average, Tn10p  
 262 and Tn10p



264 Figure 4: Spatial Distributions of Nighttime Temperature Extreme Events over West Africa (Note: n =  
 265 negative trends, n\* = negative trends significance at 0.05 alpha level, p = positive trends, p\* = positive trends  
 266 significance at 0.05 alpha level).



268 Figure 5: Spatial Distributions of Daytime Temperature Extreme Events over West Africa (Note: n = negative  
 269 trends, n\* = negative trends significance at 0.05 alpha level, p = positive trends, p\* = positive trends  
 270 significance at 0.05 alpha level, nt = no trends).

271 Table 3: Descriptive Statistics of Minimum Temperature Extremes for the Period of 1980 and 2015 over West  
272 African Zones

		Minimum	Maximum	Mean	Standard Deviation	10th Percentile	90th percentile	Kurtosis	Skewness
Tn10	HAR	4	59	36.50	13.75	18.40	55.00	-0.20	-0.44
	ARD	7	60	36.56	13.69	19.40	54.80	-0.67	-0.21
	SAR	8	59	36.53	13.69	15.80	56.30	-0.46	-0.24
	SHD	5	70	36.56	16.86	17.40	63.00	-0.69	0.15
	SHH	4	72	36.56	15.38	17.80	55.30	0.16	0.34
	HUM	0	114	36.53	30.78	2.70	86.40	0.58	1.06
Tn90	HAR	0	63	37.00	18.91	6.00	59.30	-0.96	-0.43
	ARD	7	63	36.50	14.51	11.70	55.00	-0.51	-0.39
	SAR	4	57	36.50	13.44	10.70	51.00	0.38	-0.97
	SHD	0	135	36.53	32.82	4.40	87.60	0.83	1.16
	SHH	0	86	36.53	22.70	7.20	73.30	-0.51	0.43
	HUM	0	115	36.53	34.73	0.70	98.90	-0.23	1.01
Tnn	HAR	6.48	11.92	9.43	1.28	7.81	11.12	-0.47	-0.07
	ARD	10.40	15.31	12.89	1.24	10.94	14.74	-0.60	-0.06
	SAR	13.69	18.15	16.32	1.14	14.33	17.82	0.05	-0.68
	SHD	7.73	13.36	10.67	1.34	8.91	12.76	-0.26	0.12
	SHH	16.85	21.58	19.21	1.12	17.79	20.74	-0.49	0.16
	HUM	19.78	23.32	21.63	0.94	20.31	22.99	-0.67	-0.11
Tnx	HAR	30.41	35.52	32.14	0.77	31.34	32.73	10.62	2.14
	ARD	31.55	33.83	32.85	0.49	32.24	33.57	0.41	-0.41
	SAR	31.30	34.48	33.15	0.78	31.99	34.17	-0.24	-0.36
	SHD	23.64	26.47	24.81	0.53	24.18	25.44	1.69	0.52
	SHH	26.96	29.39	28.19	0.59	27.42	29.09	-0.56	0.19
	HUM	25.67	27.67	26.68	0.51	25.99	27.46	-0.49	0.17

273

274

275

276



277 Table 4: Descriptive Statistics of Maximum Temperature Extremes for the Period of 1980 and 2015 over  
278 West African Zones

		Minimum	Maximum	Mean	Standard Deviation	10th Percentile	90th percentile	Kurtosis	Skewness
Tx10	HAR	4	60	36.56	14.11	15.50	53.00	-0.42	-0.59
	ARD	5	58	36.53	13.31	18.10	53.90	0.13	-0.51
	SAR	10	70	36.53	15.56	13.10	55.50	-0.37	0.10
	SHD	3	67	36.56	16.11	17.80	56.30	-0.80	-0.10
	SHH	0	101	36.53	25.02	8.00	75.60	-0.04	0.81
	HUM	3	96	36.42	26.27	4.00	72.60	-0.54	0.61
Tx90	HAR	7	57	36.47	14.07	16.10	55.60	-0.83	-0.40
	ARD	8	60	36.47	12.15	21.00	52.20	-0.35	-0.11
	SAR	10	64	36.53	13.97	12.70	51.90	-0.43	-0.24
	SHD	0	98	36.53	25.08	7.40	75.20	-0.22	0.68
	SHH	4	85	36.53	19.27	14.00	65.00	0.11	0.62
	HUM	1	114	36.50	27.80	9.00	77.20	1.33	1.19
Txn	HAR	12.20	18.45	15.43	1.60	13.27	18.00	-0.38	0.11
	ARD	16.63	22.69	19.30	1.44	17.05	21.08	-0.27	-0.09
	SAR	20.03	26.60	23.82	1.51	21.80	25.52	0.42	-0.62
	SHD	12.91	18.44	15.27	1.23	13.41	17.09	0.61	0.47
	SHH	25.09	29.79	28.19	1.05	26.48	29.17	1.90	-1.43
	HUM	22.63	25.78	25.05	0.64	24.15	25.65	5.44	-2.06
TxX	HAR	38.60	40.63	39.61	0.46	38.97	40.20	0.18	-0.23
	ARD	38.92	40.88	39.92	0.41	39.39	40.42	0.17	-0.22
	SAR	38.76	42.34	40.34	0.73	39.30	41.39	0.58	0.41
	SHD	26.90	29.74	28.32	0.69	27.51	29.44	-0.30	0.21
	SHH	36.11	38.82	37.42	0.69	36.58	38.49	-0.42	0.33
	HUM	29.93	32.39	31.00	0.58	30.36	31.78	-0.23	0.46

279

280 showed decreasing trends in all the six zones and the entire West Africa average (WAF) out which  
281 the SHH zone and WAF were significant for Tn10p while the SAR and SHH zones were significant  
282 for Tx10p indices (Table 5b). The decreasing trends detected for cold nights and cold days are in  
283 agreement with global and regional trends adapted from Alexander et al.(2006) and Aguilar et  
284 al.(2009) respectively. Meanwhile, increasing trends were detected for Tn90 and Tx90 indices out

which majority showed significant trends as shown in Table 5a, Figures 4b and 5b. A few exceptions were found in some parts of Nigeria, Togo, Ghana, Guinea, and Guinea-Bissau where Tx90p showed decreasing trends (Figure 5b). The increasing trends detected for warm nights and warm days are also in agreement with global and regional trends adapted from Alexander et al.(2006) and Aguilar et al.(2009) respectively.

Table 5a: Occurrence of Trends in Net Radiation and Climate Extreme Events for the Period of 1980 and 2015 over West African Zones

Variable		No of Stations	n	n*	p	p*	nt
Net Radiation	Night	45	10	2	25	8	0
	Day	45	11	25	6	3	0
	Daily	45	8	24	8	5	0
Climate Sensitivity	Daily	45	7	5	9	24	0
Extreme Temperature Event	Tn10	45	31	14	0	0	0
	Tn90	45	0	0	10	35	0
	Tnn	45	5	0	30	10	0
	Tnx	45	0	0	17	28	0
	Tx10	45	43	1	0	0	1
	Tx90	45	7	0	11	27	0
	Txn	45	13	1	20	10	1
	Txx	45	0	0	19	26	0

**Note:** n = negative trends, n\* = negative trends significance at 0.05 alpha level, p = positive trends, p\* = positive trends significance at 0.05 alpha level, nt = no trends.

Table 5b: Regional Trend Analysis of Net Radiation, Temperature and Precipitation Extreme Indices over West Africa.

Variable	Index	Mann-Kendall Trend Test ( 1980 -2015)							
		HAR	ARD	SAR	SHD	SHH	HUM	WAF	GLB
Net Radiation	Qn	1.27	1.04	-2.96*	1.44	0.41	0.35	-1.05	-
	Qx	-0.90	1.55	3.34	-2.92*	-4.60	-4.93	-2.25*	-
	Q	0.05	2.23*	2.60*	-2.94*	-4.47	-4.79	-2.77*	-
Climate Sensitivity	Φ	0.07	-2.11*	0.75	3.17*	4.51*	4.86*	3.85*	-
Temperature Extremes	Tn10	-1.01	-0.90	-0.37	-1.00	-2.75*	-3.71	-2.60*	-1.26*
	Tn90	4.85	4.13*	2.97*	4.62	2.68*	2.97*	4.48	1.58*
	Tx10	-1.34	-1.09	-1.80*	-1.40	-3.11*	-4.42	-3.57	-0.62*
	Tx90	3.42	1.73	2.88*	3.77	2.64*	1.31	3.90	0.89*
	Tnn	2.25*	2.19*	0.67	0.99	2.25*	2.27*	2.57*	0.37
	Tnx	2.03*	1.85*	0.37	0.34	1.62	3.28*	1.54	0.71*
	Txn	3.80	2.59*	3.15*	3.96	2.67*	3.01*	4.18	0.30*
	Txx	2.82*	1.70*	1.92*	2.52	2.44*	2.18*	3.12*	0.21*

**GLB = Global Trends Adapted from Alexander (2006). WAF = West Africa, \* Significant Trends at 0.05 alpha level.**

Similarly, increasing trends were detected out which majority showed significant trends for Tnn, Tnx, Txn, Txx over West Africa as shown in Table 5a, Figures 4c 4d, 5c, and 5d. On the regional average, Tnn and Tnx showed significant increasing trends in all the six zones and the entire West Africa average (WAF) except in the SAR and SHD zones for coldest nights (Tnn) together with the SAR, SHD and SHH zones for coldest days (Txn) indices. Tnx and Txx also showed significant increasing trends in all zones except in HAR and SHD for warmest nights (Tnx) together with SHD for warmest days (Table 5b). The predominant increasing trends detected for warmest temperatures for nights and days are in agreement with global and regional trends adapted from Alexander et al.(2006) and Aguilar et al.(2009) respectively. Consequently, an increase in warm temperature may affect the developmental stage and growth rate of both plants and humans. This can be attributed to the reduction in vegetation, area geometry, anthropogenic heat emission, clear skies, calm wind, and geographical location (Meehl and Tebaldi 2004, Robine et al. 2008, Peterson et al. 2012, Masson et al. 2014, Traiteur and Roy 2016).

Generally, the observed changes in temperature extremes indices in this study are consistent with the assessment of an increase in warm days and nights frequencies and a reduction in cold days and nights as it was also observed by Alexander et al.(2006) and Trenberth et al. (2007) on the global trends and by (Meehl et al. 2007, Aguilar et al. 2009, Kürbis et al. 2009, You et al. 2011) on regional trends reported in the Intergovernmental Panel on Climate Change (IPCC) assessment reports. The few departures from this overall behaviour towards more warming days and nights and fewer cold days and nights may be associated with a change in the hydrological cycle, soil moisture and aerosols feedbacks in agreement with Pan et al. (2004); Portmann et al. (2009) and Nicholls et al. (2012). The observations from Figures (5 – 6) and Tables 5 (a-b) revealed that changes in the frequencies of warm days and cold days showed warming which is less than those of warm nights and days in agreement with Vose et al.(2005); Alexander et al.(2006) and Trenberth et al. (2007). That is, nights are observed to be warmer than the days across all the regions in West Africa.

#### **3.4. Cross-Correlation Analysis between Radiation balance flux and Climate Extreme Events**

The time-lagged relationships between radiation balance fluxes ( $Q_x$  and  $Q_n$ ) and the changes in temperature extreme events were evaluated at a threshold value of 0.35 bound for the alpha level of significance of ( $\alpha = 0.05$ ) using the cross-correlation function (CCF) as shown in Figures 6 – 9.

##### ***Radiation Balance Flux and Temperature Extreme during the Night***

It can be observed from Figure 6 (a-d) that in the arid zone, nighttime radiation balance flux ( $Q_n$ ) has a significant relationship with: cold nights (Tn10p) at positive time-lag of 4 years upward, warm nights (Tn90p) at positive time-lag of 1 year downward, cold night temperature (Tnn) at positive time-lag of 3 years downward and warm night temperature (Tnx) at negative time-lag of 6 years upward in the Arid zone respectively. That is,  $Q_n$  is sensitive to: Tn10p which is responsive at four years, Tn90p responsive at one year and Tnn responsive at three years. It also showed a positive influence on Tn10p and Tn90p as well as a negative relationship with Tnn respectively. Sensitivity values being at positive



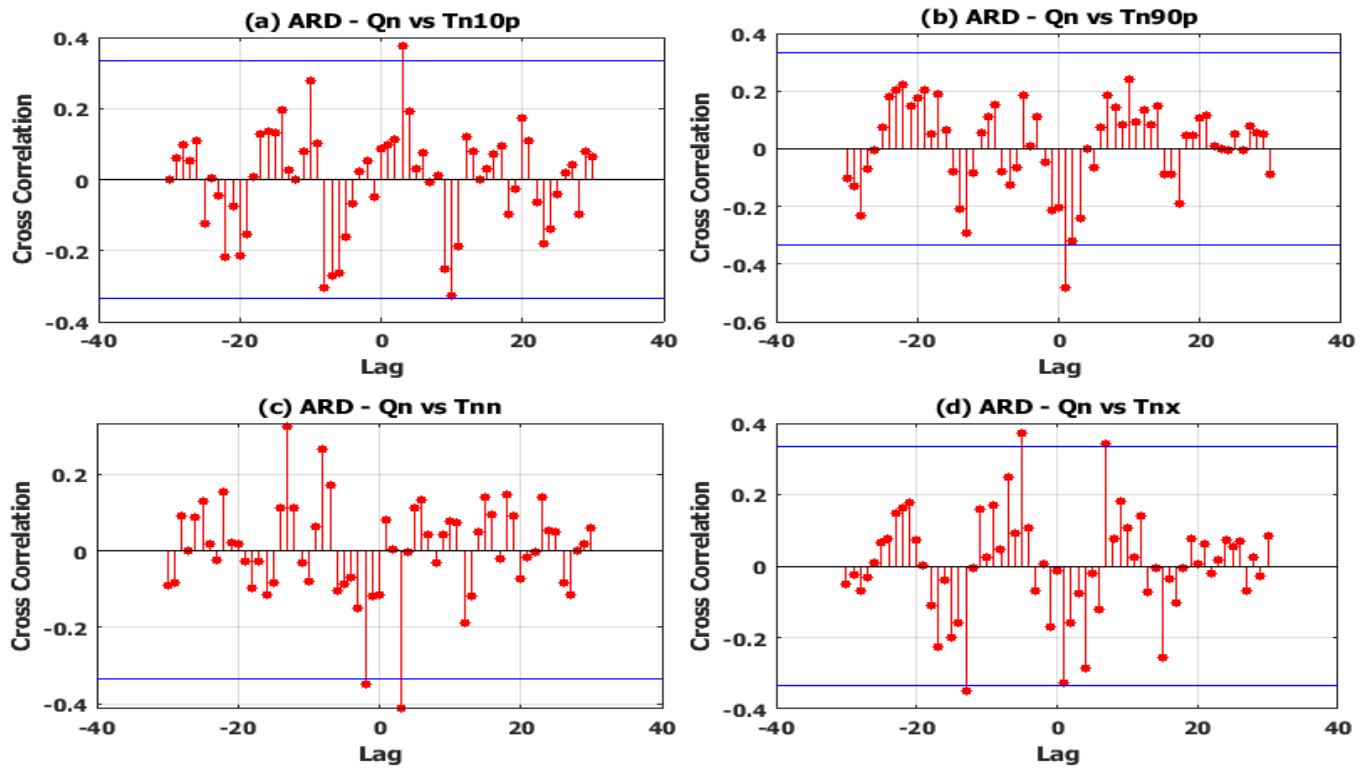


Figure 6: Cross Correlation between Nighttime Net Radiation and Cold-Warm Nights Events in the Arid Zone over West Africa

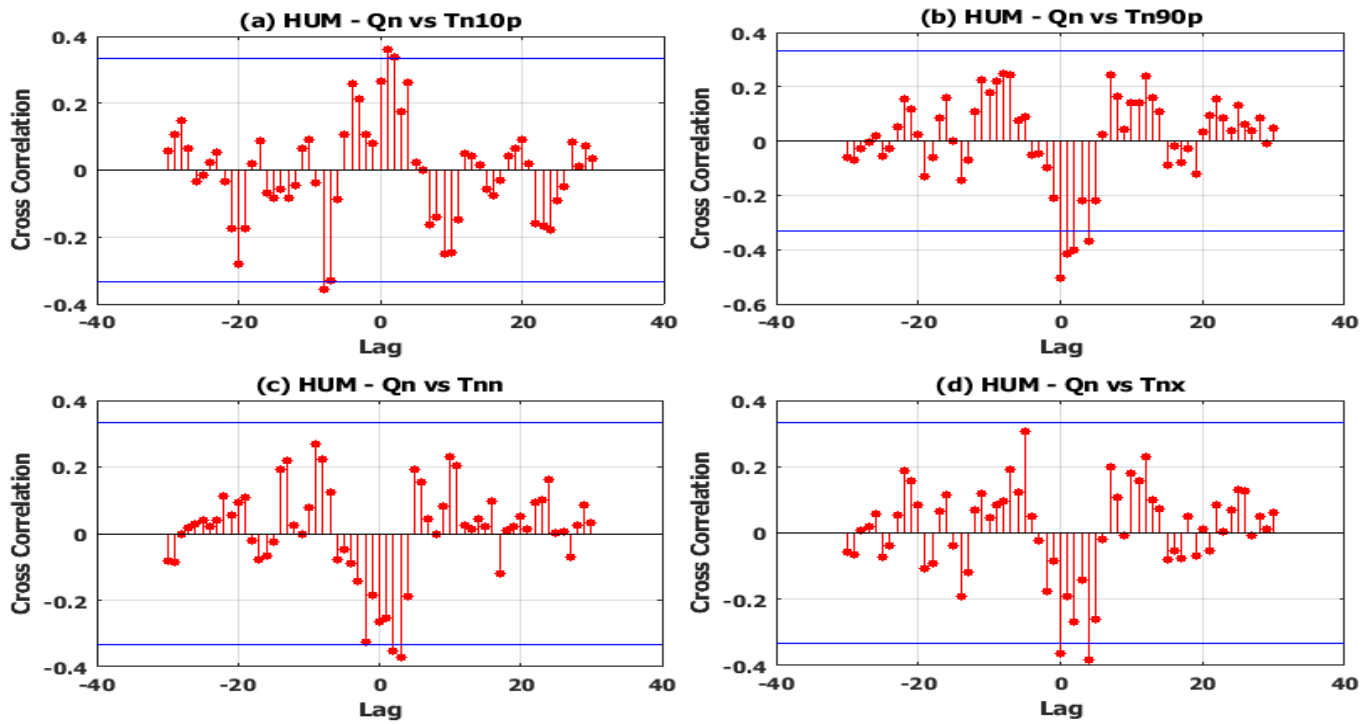


Figure 7: Cross Correlation between Nighttime Net Radiation and Cold-Warm Nights Events in the Humid Zone over West Africa

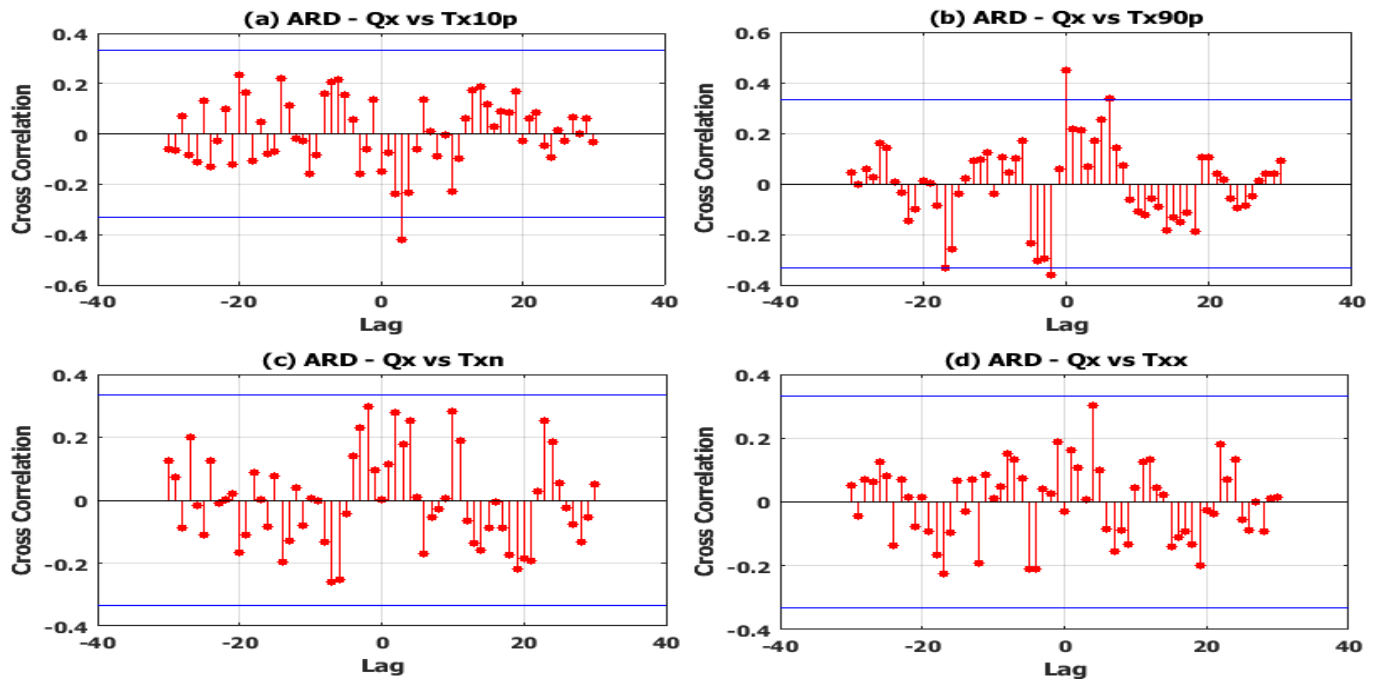


Figure 8: Cross Correlation between Daytime Net Radiation and Cold-Warm Days Events in the Arid Zone over West Africa

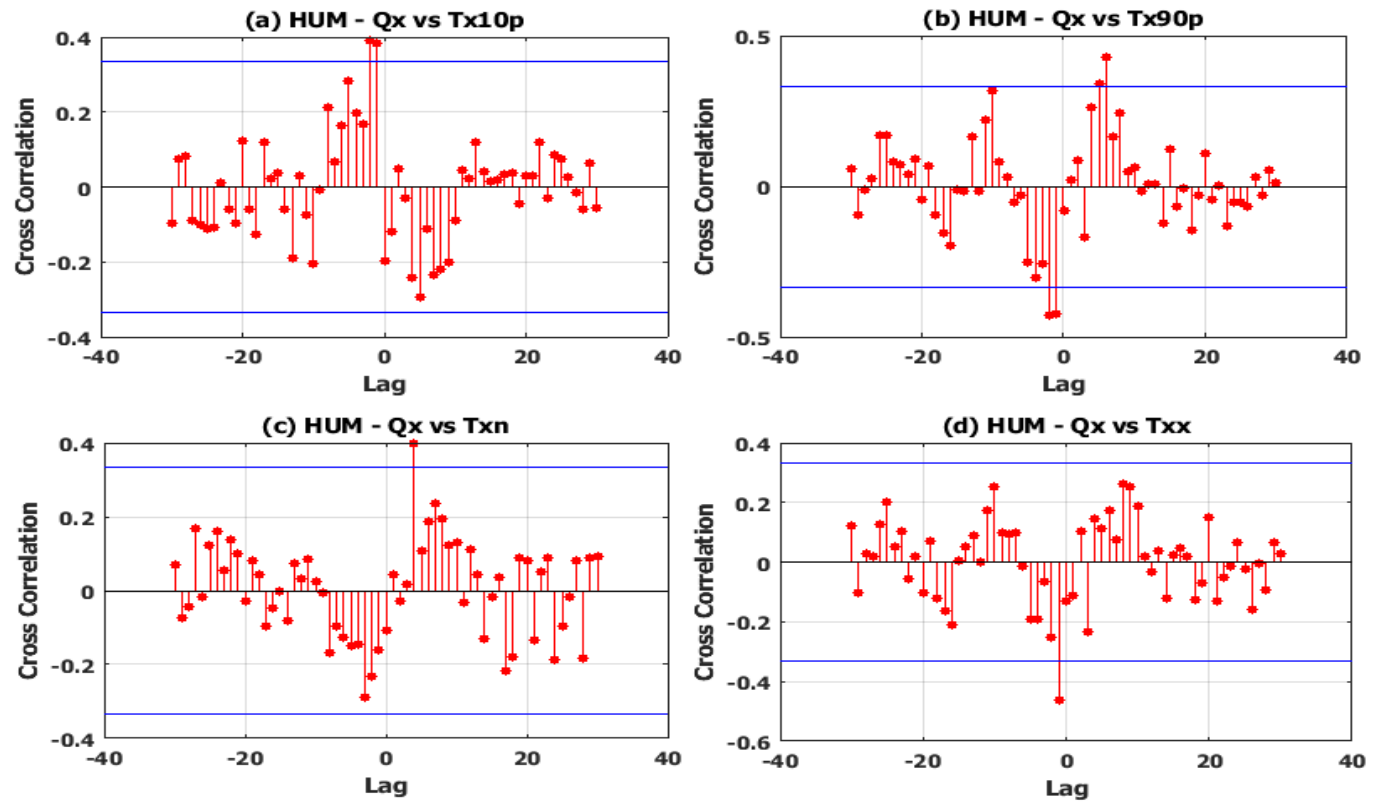


Figure 9: Cross Correlation between Daytime Net Radiation and Cold-Warm Days Events in the Humid Zone over West Africa

time-lag indicates that Qn is lagged by Tn10p, Tn90p and Tnn at the specified responsive lags in years respectively. However, Qn is observed to lead by Tnx being at negative responsive time-lag and they have positive sensitivity to each other. Similarly, in the Humid zone, from Figure 7 (a-d), Qn has a significant sensitivity to Tn10p at a positive response time-lag of 1 year upward, Tn90p at no response time-lag downward, Tnn at positive response time-lag of 3 years downward and Tnx at positive response time-lag of 4 years downward respectively. That is, all sensitivity values are at positive time-lags, then Qn is lagging by Tn10p, Tnn, and Tnx at the specified response time-lags respectively. It also has positive relationship with Tn10p and Tn 90p but negative correlation with Tnn and Tnx respectively in the humid zones. These results showed that Qn contributed significantly to the frequencies and intensities of cold and warm nights in the Arid and humid zones over West Africa.

#### ***Radiation Balance Flux and Temperature Extreme during the Day***

In the same vein, Figure 8 (a-d) revealed that daytime net radiation (Qx) has a significant positive sensitivity to cold days (Tx10p) and warm days (Tx90p) at positive response time-lag of 3 years downward and no response time-lag upward respectively. However, there is a non-significant positive sensitivity of Qx to Tnx at a negative response time-lag of 3 years upward and negative correlation of Qx with Txx at a positive response time-lag of 4 years upward in the Arid Zone. That is, Qx is lagging by Tx10p and Txx at response time-lag of three and four years showing significant positive and non-significant negative relationships with them respectively. Qx showed a significant positive correlation with Tx90p without time-lag. However, it is leading by Qx at time-lag of three years showing a non-significant negative correlation with each other being at negative response lags. Similarly, in the Humid zone as shown in Figure 9 (a-d), Qx has a significant positive peak correlation with Tx10p at negative responsive time-lag of 2 years upward, Tx90p at positive responsive time-lag of 6 years upward, Tnx at positive responsive time-lag of 4 years upward and responsive significant negative correlation with Txx negative time-lag of 1 year downward respectively. That is, Qx is leading by Tx10p at two years and Txx at one-year response time but it is lagging by Tx90 and Tnx showing a positive relationship with each of them in the Humid zone.

#### **4. Conclusion**

The influences of radiation balance flux, climate sensitivity and temperature extreme events on climate warming occurrence were examined using the trend analysis and cross-correlation function based on a 0.05 alpha level of significance. The spatial distribution analysis of radiation balance flux showed that its nighttime, daytime, and daily mean datasets decreased along increasing latitude across West Africa having higher values in the Humid zones but lower values in the Arid zones. This was attributed to the characteristic nature of their land surfaces in which those of the Humid zone absorbed more solar radiation that was incident on its surface than that of the Arid zone due to their respective surface albedos. Besides, the trend analyses of radiation balance fluxes showed predominant increasing trends during the nighttime but predominant during the daytime and for

daily mean over West Africa. These point to the fact that there are abundant longwave components especially OLR component which is one of the factors that causes enhancement of the surface temperature. This may consequently lead to surface warming event, a vital signature of climate change causing drought and alterations in hydrological cycles. The warming events were further investigated using the linear relations of surface temperature and radiation balance flux termed climate sensitivity deduced across the Arid and Humid areas of West Africa. The results were observed to have reached the threshold of warming events proposed by the latest IPCC assessment report. The climate sensitivity showed short-term decreasing trends in the Arid zones but long-term increasing trends in the Humid zones with maximum occurrence in Nigeria. Analyses of some climate extreme events showed that cold nights and cold days showed supremely decreasing trends. The predominant increasing trends were detected for warm nights and warm days over West Africa zones. Nighttime was also found to be warmer than the daytime. The results of the cross-correlation between radiation balance fluxes and temperature extreme indices showed predominant significant sensitive influences on each other at different response time-lags ranging from one year to six years. The variabilities of radiation balance flux, climate sensitivity and temperature extreme events pointed towards warming condition. Finally, it can be inferred that warming events are dependent on variability of radiation balance flux, climate sensitivity and temperature extreme events over West African geo-climatic zones. Consequently, these regions may be prone to drought in the Arid zones and flooding in some parts of the Arid and Humid zones. There may also be heat-related health hazards such as inhibition of flowering initiation, reduction in phenological development of plants, reduction of grain yield, increase water deficit, and reduction in the duration of the grain-filling period in plants. It may cause sterility, high mortality rate, heatstroke, heat cramps, fatigue, and heat swelling in human health. In conclusion, this study recommends public enlightenment on the consequences of surface warming, the greenness of the environment through afforestation, and the encouragement of organic fibres for industrial product packages to minimize the emission of greenhouse gases to the atmosphere.

## **Acknowledgement**

The authors thank NASA for making the atmospheric data used in this study available through Modern-Era Retrospective Analysis for Research and Applications, Version 2 (MERRA-2) database. The data is available through at Global Modeling and Assimilation Office (GMAO) (2015) in MERRA-2 `avg1_2d_rad_Nx:2d, 1-Hourly, Time-Averaged, Time-Averaged Single-Level, Assimilation,Radiation Diagnostics V5.12.4`, Greenbelt, MD, USA, Goddard Earth Sciences Data and Information Services Center (GES DISC)], [10.5067/Q9QMY5PBNV1T](https://doi.org/10.5067/Q9QMY5PBNV1T)

## **Conflict of Interest**

The authors hereby declare that there no conflict of interest.

## **References**

422 Aguilar, E., Aziz Barry, A., Brunet, M., Ekang, L., Fernandes, A., Massoukina, M., Mbah, J.,  
 423 Mhanda, A., Do Nascimento, D.J., Peterson, T.C., others: Changes in temperature and  
 424 precipitation extremes in western central Africa, Guinea Conakry, and Zimbabwe, 1955-2006  
 425 *Journal of Geophysical Research: Atmospheres* **114**(D2) (2009)

426 Alexander, L.V., Zhang, X., Peterson, T.C., Caesar, J., Gleason, B., Klein Tank, A.M.G., Haylock,  
 427 M., Collins, D., Trewin, B., Rahimzadeh, F., others: Global observed changes in daily climate  
 428 extremes of temperature and precipitation *Journal of Geophysical Research: Atmospheres*  
 429 **111**(D5) (2006). doi: 10.1029/2005JD006290

430 Andres, R.J., Boden, T.A., Bréon, F.-M., Ciais, P., Davis, S., Erickson, D., Gregg, J.S., Jacobson, A.,  
 431 Marland, G., Miller, J., others: A synthesis of carbon dioxide emissions from fossil-fuel  
 432 combustion (2012)

433 Boudiaf, B., Dabanli, I., Boutaghane, H., Şen, Z.: Temperature and Precipitation Risk Assessment  
 434 Under Climate Change Effect in Northeast Algeria *Earth Syst Environ* **4**(1), 1–14 (2020). doi:  
 435 10.1007/s41748-019-00136-7

436 Boyd, D.W.: Stochastic Analysis. In: Boyd, D.W. (ed) *Systems analysis and modeling: A macro to*  
 437 *micro approach with multidisciplinary applications* / Donald W. Boyd, pp. 211–227. Academic  
 438 Press, San Diego, CA (2001)

439 Chen, J., Liu, Y., Zhang, M., Peng, Y.: New understanding and quantification of the regime  
 440 dependence of aerosol-cloud interaction for studying aerosol indirect effects *Geophys. Res. Lett.*  
 441 **43**(4), 1780–1787 (2016). doi: 10.1002/2016GL067683

442 Croke, B., Cornish, P., Islam, A.: Modeling the Impact of Watershed Development on Water  
 443 Resources in India. In: Reddy, V.R., Syme, G.J. (eds) *Integrated assessment of scale impacts of*  
 444 *watershed intervention: Assessing hydrogeological and bio-physical influences on livelihoods*,  
 445 pp. 99–148. Elsevier, Amsterdam (2015)

446 Cryer, J.D., Chan, K.-S. (eds): *Time series analysis: With applications in R*, 2nd edn. Springer Texts  
 447 in Statistics. Springer, New York (2008)

448 Dickinson, R.E., Cicerone, R.J.: Future global warming from atmospheric trace gases *Nature*  
 449 **319**(6049), 109–115 (1986)

450 Drake, F.: *Global Warming: The Science of Climate Change* (Hodder Arnold Publication). Oxford  
 451 University Press Inc., 198 Madison Avenue, New York, NY10016 (2000)

452 Folland, C.K., Karl, T.R., Christy, JR, Clarke, R.A., Gruza, G.V., Jouzel, J., Mann, M.E.,  
 453 Oerlemans, J., Salinger, M.J., Wang, S.W., others: Observed climate variability and change  
 454 *Climate change* **2001**, 99 (2001)

455 Gilbert, R.O.: Statistical methods for environmental pollution monitoring. John Wiley & Sons  
456 (1987)

457 Gregory, J.M., Stouffer, R.J., Raper, S.C.B., Stott, P.A., Rayner, N.A.: An observationally based  
458 estimate of the climate sensitivity *Journal of Climate* **15**(22), 3117–3121 (2002)

459 Gregory, J.M., Ingram, W.J., Palmer, M.A., Jones, G.S., Stott, P.A., Thorpe, R.B., Lowe, J.A.,  
460 Johns, T.C., Williams, K.D.: A new method for diagnosing radiative forcing and climate  
461 sensitivity *Geophys. Res. Lett.* **31**(3) (2004)

462 Gröger, J.P., Fogarty, M.J.: Broad-scale climate influences on cod (*Gadus morhua*) recruitment on  
463 Georges Bank *ICES Journal of Marine Science* **68**(3), 592–602 (2011). doi:  
464 10.1093/icesjms/fsq196

465 Gröger, J.P., Kruse, G.H., Rohlf, N.: Slave to the rhythm: How large-scale climate cycles trigger  
466 herring (*Clupea harengus*) regeneration in the North Sea *ICES Journal of Marine Science* **67**(3),  
467 454–465 (2010). doi: 10.1093/icesjms/fsp259

468 Hansen, J., Sato, M., Ruedy, R., Lacis, A., Oinas, V.: Global warming in the twenty-first century: An  
469 alternative scenario *Proceedings of the National Academy of Sciences* **97**(18), 9875–9880 (2000)

470 Hansen, J.E., Sato, M.: Paleoclimate implications for human-made climate change. In: *Climate*  
471 *change*, pp. 21–47. Springer (2012)

472 Houghton, A., Castillo-Salgado, C.: Analysis of correlations between neighborhood-level  
473 vulnerability to climate change and protective green building design strategies: A spatial and  
474 ecological analysis *Building and Environment* **168**, 106523 (2020). doi:  
475 10.1016/j.buildenv.2019.106523

476 Houghton, J.T., Meira Filho, L.G., Bruce, J.P., Lee, H., Callander, B.A., Haites, E.F.: *Climate*  
477 *change 1994: Radiative forcing of climate change and an evaluation of the IPCC 1992 IS92*  
478 *emission scenarios*. Cambridge University Press (1995)

479 Jackson, L.E., Wheeler, S.M., Hollander, A.D., O’Geen, A.T., Orlove, B.S., Six, J., Sumner, D.A.,  
480 Santos-Martin, F., Kramer, J.B., Horwath, W.R., others: Case study on potential agricultural  
481 responses to climate change in a California landscape *Climatic Change* **109**(1), 407–427 (2011)

482 Kamata, Y., Matsunami, A., Kitagawa, K., Arai, N.: FFT analysis of atmospheric trace concentration  
483 of N<sub>2</sub>O continuously monitored by gas chromatography and cross-correlation to climate  
484 parameters *Microchemical Journal* **71**(1), 83–93 (2002). doi: 10.1016/S0026-265X(01)00140-0

485 Keggenhoff, I., Elizbarashvili, M., Amiri-Farahani, A., King, L.: Trends in daily temperature and  
 486 precipitation extremes over Georgia, 1971–2010 *Weather and Climate Extremes* **4**, 75–85  
 487 (2014). doi: 10.1016/j.wace.2014.05.001

488 Kürbis, K., Mudelsee, M., Tetzlaff, G., Brázdil, R.: Trends in extremes of temperature, dew point,  
 489 and precipitation from long instrumental series from central Europe *Theor Appl Climatol* **98**(1-  
 490 2), 187–195 (2009). doi: 10.1007/s00704-008-0094-5

491 Lal, R.: Soil carbon sequestration impacts on global climate change and food security science  
 492 **304**(5677), 1623–1627 (2004)

493 Laurance, W.F., Williamson, G.B.: Positive feedbacks among forest fragmentation, drought, and  
 494 climate change in the Amazon *Conservation biology* **15**(6), 1529–1535 (2001)

495 Liang, S., Wang, D., He, T., Yu, Y.: Remote sensing of earth’s energy budget: Synthesis and review  
 496 *International Journal of Digital Earth* **12**(7), 737–780 (2018). doi:  
 497 10.1080/17538947.2019.1597189

498 Lin, B., Min, Q., Sun, W., Hu, Y., Fan, T.-F.: Can climate sensitivity be estimated from short-term  
 499 relationships of top-of-atmosphere net radiation and surface temperature? *Journal of Quantitative*  
 500 *Spectroscopy and Radiative Transfer* **112**(2), 177–181 (2011). doi: 10.1016/j.jqsrt.2010.03.012

501 Maslin, M.: *Global Warming: A Very Short Introduction*. Oxford University Press Inc., (2004)

502 Masson, V., Marchadier, C., Adolphe, L., Aguejdad, R., Avner, P., Bonhomme, M., Bretagne, G.,  
 503 Briottet, X., Bueno, B., Munck, C. de, others: Adapting cities to climate change: A systemic  
 504 modelling approach *Urban Climate* **10**, 407–429 (2014)

505 Meehl, G.A., Tebaldi, C.: More intense, more frequent, and longer lasting heat waves in the 21st  
 506 century science **305**(5686), 994–997 (2004). doi: 10.1126/science.1098704

507 Meehl, G.A., Covey, C., Delworth, T., Latif, M., McAvaney, B., Mitchell, J.F.B., Stouffer, R.J.,  
 508 Taylor, K.E.: The WCRP CMIP3 multimodel dataset: A new era in climate change research  
 509 *Bulletin of the American meteorological society* **88**(9), 1383–1394 (2007)

510 Menke, W., Menke, J.: Detecting correlations among data. In: Menke, W., Menke, J.E. (eds)  
 511 *Environmental data analysis with MatLab*, pp. 187–221. Elsevier Academic Press, Amsterdam,  
 512 Boston (2016)

513 Nicholls, N., Seneviratne, S., Reichstein, M., Sorteberg, A., Vera, C., Zhang, X.: Changes in Climate  
 514 Extremes and their Impacts on the 1 Natural Physical Environment 2. In: Matilde Rusticucci  
 515 (Argentina), Vladimir Semenov (Russia) (ed) *Managing the risks of extreme events and disasters*  
 516 *to advance climate change adaptation: Changes in Climate Extremes and their Impacts on the*

517 Natural Physical Environment, pp. 109–230. Cambridge University Press Cambridge, UK, and  
518 New York, NY, USA (2012)

519 Ogolo, E.O., Adeyemi, B.: Variations and trends of some meteorological parameters at Ibadan,  
520 Nigeria The Pacific Journal of Science and Technology **10**(2), 981–987 (2009)

521 Ojo, O.S., Adeyemi, B., Ogolo, E.O.: Assessments of the night-time and daytime radiative fluxes  
522 balance on seasonal timescale over West Africa Journal of Atmospheric and Solar-Terrestrial  
523 Physics **191**, 105048 (2019)

524 Pan, Z., Arritt, R.W., Takle, E.S., Gutowski, W.J., Anderson, C.J., Segal, M.: Altered hydrologic  
525 feedback in a warming climate introduces a “warming hole” Geophys. Res. Lett. **31**(17), n/a-n/a  
526 (2004). doi: 10.1029/2004GL020528

527 Peterson, T.C., Stott, P.A., Herring, S.: Explaining extreme events of 2011 from a climate  
528 perspective Bulletin of the American meteorological society **93**(7), 1041–1067 (2012)

529 Portmann, R.W., Solomon, S., Hegerl, G.C.: Spatial and seasonal patterns in climate change,  
530 temperatures, and precipitation across the United States Proceedings of the National Academy of  
531 Sciences **106**(18), 7324–7329 (2009). doi: 10.1073/pnas.0808533106

532 Probst, W.N., Stelzenmüller, V., Fock, H.O.: Using cross-correlations to assess the relationship  
533 between time-lagged pressure and state indicators: An exemplary analysis of North Sea fish  
534 population indicators ICES Journal of Marine Science **69**(4), 670–681 (2012). doi:  
535 10.1093/icesjms/fss015

536 Rahmstorf, S.: Anthropogenic climate change: Revisiting the facts Global Warming: Looking  
537 Beyond Kyoto, 34–53 (2008)

538 Rannow, S., Neubert, M.: Managing protected areas in Central and Eastern Europe under climate  
539 change. Advances in global change research, 1574-0919, volume 58. Springer, Dordrecht (2014)

540 Rice, J.C., Rochet, M.-J.: A framework for selecting a suite of indicators for fisheries management  
541 ICES Journal of Marine Science **62**(3), 516–527 (2005). doi: 10.1016/j.icesjms.2005.01.003

542 Robine, J.-M., Cheung, S.L.K., Le Roy, S., van Oyen, H., Griffiths, C., Michel, J.-P., Herrmann,  
543 F.R.: Death toll exceeded 70,000 in Europe during the summer of 2003 Comptes rendus  
544 biologies **331**(2), 171–178 (2008)

545 Rohling, E.J., Sluijs, A., Dijkstra, H.A., Köhler, P., van de Wal, R.S.W., Heydt, A.S. von der,  
546 Beerling, D.J., Berger, A., Bijl, P.K., Crucifix, M., others: Making sense of palaeoclimate  
547 sensitivity Nature **491**(7426), 683–691 (2012)



548 Sai Krishna, S.V.S., Manavalan, P., Rao, P.V.N.: Estimation of Net Radiation using satellite based  
549 data inputs Int. Arch. Photogramm. Remote Sens. Spatial Inf. Sci. **XL-8**, 307–313 (2014). doi:  
550 10.5194/isprsarchives-XL-8-307-2014

551 Saud, T., Dey, S., Das, S., Dutta, S.: A satellite-based 13-year climatology of net cloud radiative  
552 forcing over the Indian monsoon region Atmospheric Research **182**, 76–86 (2016). doi:  
553 10.1016/j.atmosres.2016.07.017

554 Schwarzkopf, M.D., Ramaswamy, V.: Radiative forcing due to ozone in the 1980s: Dependence on  
555 altitude of ozone change Geophys. Res. Lett. **20**(3), 205–208 (1993)

556 Seo, S.B., Das Bhowmik, R., Sankarasubramanian, A., Mahinthakumar, G., Kumar, M.: The role of  
557 cross-correlation between precipitation and temperature in basin-scale simulations of hydrologic  
558 variables Journal of Hydrology **570**, 304–314 (2019). doi: 10.1016/j.jhydrol.2018.12.076

559 Song, H.: Review of Time Series Analysis and Its Applications With R Examples (3rd Edition) , by  
560 Robert H. Shumway & David S. Stoffer Structural Equation Modeling: A Multidisciplinary  
561 Journal **24**(5), 800–802 (2017). doi: 10.1080/10705511.2017.1299578

562 Traiteur, J.J., Roy, S.B.: Impacts of Wind Farms on Weather and Climate at Local and Global Scales  
563 Alternative Energy and Shale Gas Encyclopedia, 88 (2016)

564 Trenberth, K.E., Jones, P.D., Ambenje, P., Bojariu, R., Easterling, D., Tank, A.K., Parker, D.,  
565 Rahimzadeh, F., Renwick, J.A., Rusticucci, M., others: Observations: Surface and atmospheric  
566 climate change., 235–336 (2007)

567 Trenberth, K.E., Fasullo, J.T., Balmaseda, M.A.: Earth’s energy imbalance Journal of Climate **27**(9),  
568 3129–3144 (2014)

569 Tung, K.K., Zhou, J., Camp, C.D.: Constraining model transient climate response using independent  
570 observations of solar-cycle forcing and response Geophys. Res. Lett. **35**(17) (2008)

571 Vose, R.S., Easterling, D.R., Gleason, B.: Maximum and minimum temperature trends for the globe:  
572 An update through 2004 Geophys. Res. Lett. **32**(23) (2005)

573 You, Q., Kang, S., Aguilar, E., Pepin, N., Flügel, W.-A., Yan, Y., Xu, Y., Zhang, Y., Huang, J.:  
574 Changes in daily climate extremes in China and their connection to the large scale atmospheric  
575 circulation during 1961–2003 Clim Dyn **36**(11-12), 2399–2417 (2011). doi: 10.1007/s00382-  
576 009-0735-0

577 Zhang, H., Zhai, P.: Temporal and spatial characteristics of extreme hourly precipitation over eastern  
578 China in the warm season Advances in atmospheric sciences **28**(5), 1177 (2011)

